ABSOLUTE RADIOMETRIC CALIBRATION OF ADVANCED REMOTE SENSING SYSTEMS

P. N. Slater

Committee on Remote Sensing
Optical Sciences Center
University of Arizona

ABSTRACT

The distinction between the uses of relative and absolute spectroradiometric calibration of remote sensing systems is discussed. The advantages of detector-based absolute calibration are described, and the categories of relative and absolute system calibrations are listed. The limitations and problems associated with three common methods used for the absolute calibration of remote sensing systems are discussed.

Two methods are proposed for the in-flight absolute calibration of advanced multispectral linear array (MLA) systems. One makes use of a sun-illuminated panel in front of the sensor, the radiance of which is monitored by a spectrally flat pyroelectric radiometer. The other uses a large, uniform, high-radiance reference ground surface. The ground and atmospheric measurements required as input to a radiative transfer program to predict the radiance level at the entrance pupil of the orbital sensor are discussed, and the ground instrumentation is described.

Key words: Radiometry; Calibration; Remote Sensing.

1. SPECTRORADIOMETRIC CALIBRATION--WHO NEEDS IT?

For purposes of this discussion, the community of remote sensing data users can be divided into two groups :

1. Users requiring relative, but not necessarily absolute, spectroradiometric sensor calibration. These include workers in computer-aided scene classification, cartographers, image processors, photointerpreters, and people concerned with composing large mosaics.

2. Users requiring absolute spectro-radiometric calibration. These include physical scientists concerned with relating ground-measured parameters and/or atmospheric characteristics to the spectral radiance at the entrance pupil of the space sensor.

The distinction can be drawn that the former are concerned primarily with taking an inventory or compiling a map of ground features. The latter are concerned primarily with understanding and characterizing the physical interactions taking place, usually through models and often with a view to optimizing (for example an irrigation schedule) or to predicting a change in a particular process (for example an agricultural yield). Expressed differently, those concerned with relative calibration use data described in digital counts, while those needing absolute calibration use data referenced in terms of radiance units at the entrance pupil of the sensor (in this case, the radiometric calibration of the sensor is invoked to convert the digital value to spectral radiance). We must emphasize that the radiance value is of no more worth to the average user than the digital value, as both refer to an incident radiance level at the sensor over broad, unequal spectral passbands, over which the spectral reflectance of the feature being observed can change by a significant but unknown amount. However, there are two reasons for converting the digital value to radiance: first, in multitemporal sensing, to account for any documented changes of radiometric calibration with time; second, to test or utilize physical models in which the ground reflectance and atmospheric effects are measured and/or calculated over identical spectral passbands as employed by the space sensor.

Perfect relative radiometric response occurs when the outputs from all detectors in a band are equal or can be adjusted during preprocessing to be equal, when the incident spectral radiance is constant across the sensor's field of view. (Note that the number of detectors in a band can be as few as six for the Multispectral Scanner System (MSS) on Landsat and as many as 18,500 on future MLA systems.) This condition must be met independently of the spectral content of the scene. When this condition is not met, the image appears striped. If it is not scene-dependent, striping often can be completely removed by the histogram equalization method; thus, relative radiometric precision can be high even though the accuracy involved may be low. In this equalization procedure the histogram of each detector output is compared with that of every other detector, after a large number of data samples ($\sim 2 \times 10^5$) have been recorded. It is assumed that, if the scene is spatially and spectrally random, the histograms for a large number of samples will be identical. If the histograms are not identical, adjustments are made during the preprocessing step to make them so. This procedure can be repeated for scenes of different average radiance, and the relative responses can then be equalized over the dynamic range of the detectors. This procedure does not work if the striping is scene-dependent (Ref. 1). Fortunately the design and the spectral band location for the Thematic Mapper and future MLA sensors will not give rise to a scene-dependent

striping problem of the magnitude of that in the MSS.

Inadequately corrected relative detector-to-detector response causes unsightly striping in the imagery. Striping can cause inaccuracies in automated scene classification. In addition, even though the human photointerpreter is usually more forgiving than a computer, if the striping is severe it can cause errors in photointerpretation. Uncorrected striping can be aggravated by the application of some image processing algorithms. Thus, it is important to reduce striping as much as possible for image processing and classification purposes. The relative response of the individual detectors is also important for ratioing purposes. However, once the in-band tolerance has been met, the concern is with the relative stability of response because many applications utilize the comparison of multitemporal band ratios.

The utilization or verification of physical models usually requires the use of data calibrated in an absolute sense. Until recently the highest in-orbit absolute radiometric accuracy has been little better than 10%. This low accuracy has been due to: (a) the fact that the calibration in orbit has often been for the focal plane only, not for the complete system; (b) the loss in accuracy accompanying the transfer of calibration from the standard source at the national laboratory to the factory or laboratory calibration site; (c) the use of source-based calibration procedures.

As described later, the use of detector-based calibration promises to reduce the approximately 10% error to 1%. To what extent we can afford to relax or strive to exceed the 1% potential can best be determined from a set of well-coordinated measurement and modeling exercises conducted as part of an experimental MLA mission. The results of work to date on this subject are in disagreement. On one hand we know that natural or scene variability is seldom less than 1% and we also know from atmospheric modeling work (not yet experimentally verified) that we can expect considerable atmospheric-scatter-induced spectral radiance crosstalk between neighboring ground samples owing to the so-called adjacency or boundary effect (Refs. 2-5). On the other hand, the sensor simulations made to date (Ref. 6) indicate there is an improvement in classification accuracy in going from 6-bit to 8-bit quantization. Eight-bit quantization is available on most future sensors. A purist might contend that, if 8-bit radiometric resolution is really justified, it should, for maximum utility, be associated with commensurate (<0.4%) error in absolute radiometric accuracy!

In summary, we know that spectroradiometric calibration is important and that the need for relative or absolute calibration depends on the application for the data. However, we do not know how accurate the calibrations should be, particularly the absolute calibration. The most encouraging aspect of the situation is that we now have the potential of utilizing 8-bit quantization resolution with commensurate absolute radiometric accuracy in an orbital imager at least over the 400 to 900 nm range. This potential should be exploited as fully as possible as an important component of any system and applications research associated with an experimental land-observing system having an 8- to 10-bit quantization capability.

2. DETECTOR-BASED RADIOMETRIC CALIBRATION

The recent work at the US National Bureau of Standards on self-calibrated photodiodes is described only briefly here. For more details the interested reader is referred to references 7-12.

The calibration of the photodiode is accomplished by either of two differently applied biasing procedures, depending on the wavelength region of interest. At short wavelengths, a negative bias is applied to remove the recombination centers at the Si-SiO interface at the front of the detector. To do this, a contact is made with the front surface using an electrode immersed in a conducting liquid, or the surface can be exposed to a corona discharge. For long wavelengths, a back-bias is applied to extend the depletion region to a depth beyond which incident flux penetrates. The experimental procedure is to irradiate the detector with a constant monochromatic flux level and to increase the bias voltage until further increase no longer gives rise to an increase in output signal. For both the short and the long wavelength ranges, the internal quantum efficiency saturates at a value extremely close to unity, as shown in Fig. 1. Thus the maximum increase in signal output obtained as a result of biasing can be used to determine the internal quantum efficiency of the detector without biasing, as it will be used in practice.

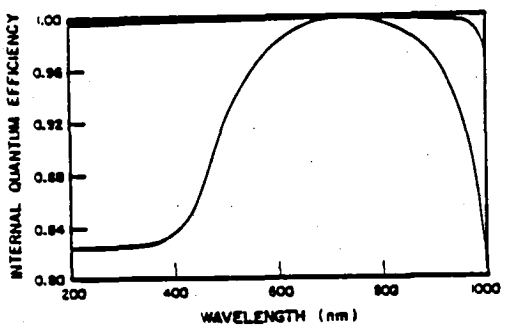

Fig. 1. Typical photodiode internal quantum efficiency without biasing (lower curve) and with biasing (upper curve), reference 9.

The only significant loss in the external quantum efficiency of the photodiode is caused by reflection. This can be reduced to insignificance by making use of three photodiodes according to the geometry sketched in Fig. 2.

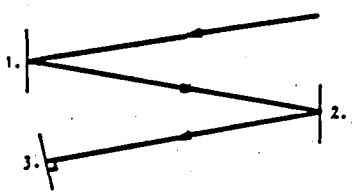

Fig. 2. A three-diode arrangement to minimize specular reflection losses.

The output signals from the three diodes are summed to provide the signal corresponding to a black detector of overall quantum efficiency that

can be assumed to be unity. The second diode reflects the specular reflection from diode 1 to diode 3, which acts as a retroreflector. The incident flux thereby undergoes five reflections, and at a 10% value the final specular reflectance is down to 10^{-5} of the initial incident radiance. It is claimed (Ref. 12) that the diffuse reflectance losses for clean detectors are typically much less than 1%. The photodiodes used in similar calibration facilities at NBS and at the University of Arizona, Optical Sciences Center, are EGG UV 444B.

The discussion at the end of this paper refers to the use of self-calibrating NBS detectors for the spectroradiometric calibration of an MLA system. However, as shown in Fig. 1, the unbiased quantum efficiency is wavelength dependent. Because of possible changes in the passband position of spectral filters during long duration space flights, it may be advisable to use the NBS detectors to calibrate a spectrally flat pyroelectric detector, at the 0.1-0.2% level, and for that to be used in the in-orbit calibration.

3. BROAD CLASSIFICATION OF CALIBRATION PROCEDURES

Some of the most commonly used procedures for the calibration of remote sensing systems are referred to in Fig. 3. The two major divisions in the figure are between relative and absolute calibration and between the static macro-image response and the dynamic micro-image response of the system. Some aspects of relative calibration were discussed in the first part of this paper and together with dynamic micro-image response will not be discussed further, beyond remarking that the dynamic micro-image response is of vital interest in any pixel-by-pixel analysis of remotely collected imagery. The rest of this paper deals with the absolute calibration of remote sensing systems, and only the static macro-image response will be considered in this context, as is usually the case.

The procedures for the absolute calibration of a remote sensing system fall into the three categories shown in the bottom right of Fig. 3:

(1) The absolute calibration of the system is made only before launch. In flight the calibration is checked by irradiating the focal plane with a radiometrically calibrated source and optical system. The drawbacks to this procedure are that any change in the transmission of the image-forming optics of the sensor system, due to the condensation of outgassed contaminants, will be undetected and the on-board calibration system is also assumed to be stable through launch and unaffected by the vacuum, high energy particle irradiation, and zero-g environment at orbital altitudes. The Thematic Mapper and the Multispectral Scanner System on Landsat-D are examples of remote sensing systems calibrated in this manner.

(2) The sun or an on-board calibrated source can be used to irradiate the focal plane through the image-forming optics. The drawbacks to this approach are the uncertainty in the knowledge of (a) the irradiance of the sun above the atmosphere and (b) the output of the calibrated source system, for the reasons mentioned earlier. Furthermore, in examples of the use of this procedure (MSSs 1, 2 and 3 and SPOT), the calibration beam passes through only a small portion of the aperture of the system, thus not simulating the actual operation of the system. When imaging the ground, the system entrance aperture is irradiated over its entire area by flux incident over a roughly three steradian solid angle. In the imaging mode there is much more stray light present in the system and incident on the focal plane. If this additional flux level is unknown, it may introduce a substantial uncertainty into the absolute calibration of the system.

(c) Reference can be made in-flight to a ground area of known spectral radiance. If at the time the sensor system is imaging the known area, measurements are made of the atmospheric conditions, these data can be used with an atmospheric radiative transfer program to predict the spectral radiance at the entrance pupil of the sensor. The main uncertainty in this approach is that of determining the atmospheric aerosol content well enough. The approach is also limited to scenes having large uniform areas of high radiance. For example, although many water bodies are of sufficient size and uniformity, they are not appropriate for calibration purposes because their radiance is too low to provide a calibration of sufficient accuracy or to cover much of the dynamic range of the sensor. Fortunately, some suitable areas do exist, particularly in the arid regions of

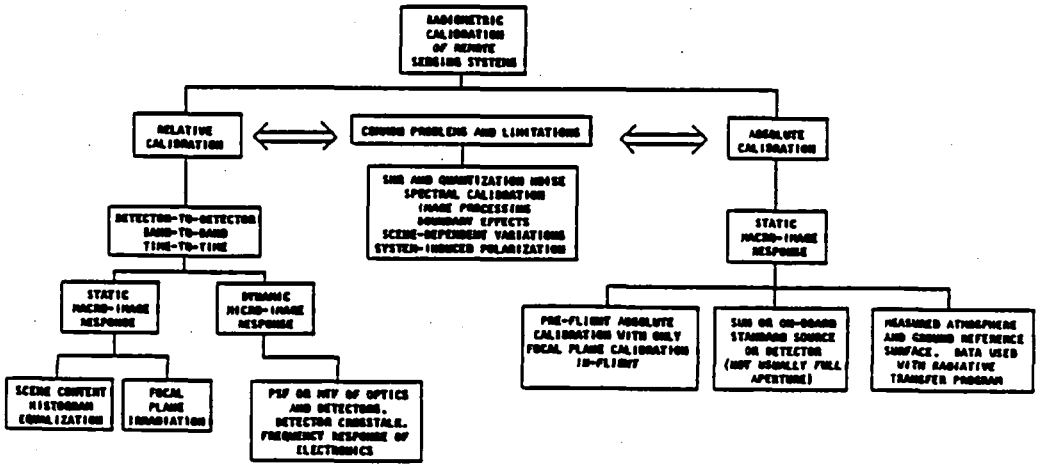

Fig. 3. Classification of radiometric calibration procedures.

the world, for example at White Sands, New Mexico, in the United States.

The rest of this paper is devoted to discussion of the factory and in-flight calibration of an MLA system using the self-calibrated photodiode approach and the use of a ground reference area for calibration purposes.

4. CALIBRATION IN THE FACTORY AND IN ORBIT

The concept proposed for the factory calibration is similar to the proposed orbital procedure, the main difference being that an artificial source is used in the factory and the sun is used in orbit—simply a matter of convenience in the former case and of convenience and reliability in the latter case. In the factory, redundancy is not at a premium and our requirements for a source are simply power, spectral flatness, and stability. We do not need a standard source although an array of standard NBS FEL tungsten halogen lamps could be used, if their polarization characteristics can be tolerated (Ref. 13). A xenon arc selected for minimum arc wander and with a highly stable power supply and a feedback loop would suffice.

The source would be used to irradiate a near-Lambertian, near-unity-reflectance, white-surfaced panel perhaps 1 m x 0.5 m in size in front of the system. (An integrating sphere could be used, but it would have to be very large, and uniformity checks can sometimes themselves introduce non-uniformities.) A self-calibrating NBS-style radiometer, with the incident beam perhaps defined by two or three apertures, and using spectral bandpass filters matching those used in the MLA, would be used to determine the radiance of the panel in each band. The MLA would image the panel out of focus, but being an extended object, its image would have exactly the same irradiance in or out of focus. The arrangement is sketched in Fig. 4.

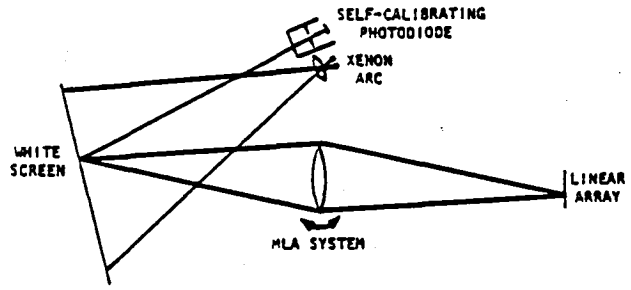

Fig. 4. The factory procedure for absolute spectroradiometric calibration.

To avoid problems due to the nonuniform irradiation of the panel, the MLA should be rotated to sequentially irradiate the focal plane with the image of the same small area that is sampled by the radiometer. The reason for a large panel is to simulate the viewing conditions from space in which, depending on the baffle design, significant out-of-the-field-of-view stray light could be incident on the image plane to modify the calibration. For this reason it would be worthwhile to conduct at least one calibration using a white panel several meters in diameter. To check for linearity of response, several different irradiance levels on the panel should be used. This irradiance level can be changed conveniently by inserting heat-resistant neutral density filters in front of the stabilized xenon arc source.

The profiles of the spectral filters should be measured in a spectrophotometer using the same F/No. beam as the MLA. If they are integral with the array, they should be measured using a double monochromator, again with the MLA F/No., before installation in the focal plane. Care should be taken to cover the whole wavelength sensitivity range of the detectors, the off-band suppression being particularly important for detectors with the wide spectral response of silicon.

The procedure proposed here for in-flight calibration is similar to the panel method sketched in Fig. 4, but it uses the sun as the source. We believe that the irradiance over the panel can then be considered to be uniform and known spectrally to better than 1% absolute. (Several solar measurement programs are currently being conducted with this accuracy as a goal. However, if the uncertainty is thought to be greater than 1%, a pyroelectric detector could be used to measure the direct solar flux in orbit, over the wavelength intervals of interest and at the same time that the system is being calibrated.) The calibration would be carried out in the few minutes while the spacecraft is sun-illuminated but before it images the sun-illuminated earth. The absolute radiometer containing the pyroelectric detector would now be needed only to check for any deterioration in the reflectance of the panel owing to exposure to the space environment and short exposures to unattenuated UV and other high energy radiation from the sun and from space. In this last respect, the panel would usually be stowed in a well-shielded compartment and exposed only during actual calibration checks. Also, when deployed, it would not interfere with normal operation of the system, as it would be viewed by the stereo mirror in one of its extreme positions. In this respect it is fail-safe.

5. WHITE SANDS AS A CALIBRATION REFERENCE

To keep the decription of the theory of the method brief, spectral dependencies are not included in the following discussion. In all cases the spectral dependence is implied, the spectral value having the same wavelength dependence as the spectral response of each band of the sensor being calibrated. The theoretical basis for the calibration method is straightforward.

The radiance at the sensor, L_s, is determined with respect to the ground radiance, L_o, the reduction of this radiance by the upward path through the atmosphere, $\tau'_{ext} \sec\theta$ (where τ'_{ext} is the atmospheric extinction and 0 is the nadir scan angle), and $L_{\theta,\phi}$, the atmospheric path radiance (where ϕ is the azimuth angle of the observation). Thus,

$$L_s = L_o \exp(\tau'_{ext} \sec\theta) + L_{\theta,\phi}$$

The path radiance term, $L_{\theta,\phi}$, in the equation is unknown and can be determined only by the use of a radiative transfer calculation. Such calculations require a knowledge of τ'_{ext}, ground reflectance, the irradiance incident at the top of the atmosphere, the aerosol optical depth and phase

function, the optical depth due to ozone and water vapor, the solar zenith angle, the nadir angle of the sensor, and its azimuthal angle with respect to the sun's direction. These radiative transfer calculations assume an infinite, flat, Lambertian reflecting surface with an atmosphere composed of plane homogeneous layers. Although these assumptions are never exactly met, they are closely approximated by the nearly Lambertian flat surface of the gypsum at White Sands and the small field of view of the space sensors.

The quantity τ'_{ext} can be determined from the solar radiometer data in the following way. The solar radiometer records the irradiance E_{θ_z} at the ground as a function of the solar zenith angle during the morning of the overpass. If the atmospheric conditions are steady during that period, the Langley plot of $\ln E_{\theta_z}$ against $\sec\theta$ is a straight line of slope τ'_{ext}. The extrapolation of the line to a $\sec\theta_z$ value of zero gives the value of the irradiance above the atmosphere in the measurement passband. The value of the ground radiance L_o is determined at the time of the overflight by the solar radiometer looking at the ground at the same θ and ϕ angles as that of the space sensor. The ground radiance value can be converted into the reflectance required as input to the radiative transfer program in one of two ways. First, the global irradiance can be measured by the solar radiometer with either a horizontal cosine diffuser or an integrating sphere, with horizontal entrance port, placed over the entrance aperture of the solar radiometer. Or second, the solar radiometer can be pointed down at a horizontal, diffusing, white surface such as $BaSO_4$ or Halon. The cosine diffuser approach is preferred because its small surface can be conveniently stored to minimize contamination. Intercomparisons will be made, during the six monthly recalibrations of the field equipment, between the cosine diffuser global irradiance and the Lambertian white reference surface measurements of the ground reflectance. The nadir angle from the satellite to the ground observation point, the solar zenith angle, and the azimuth of the satellite nadir angle to the sun's direction are all readily determinable. Such quantities as atmospheric pressure, humidity, surface and air temperature, etc., are routinely monitored by the Atmospheric Sciences Laboratory at White Sands. These data will be formatted with the radiation data and telemetered to Wallops Island, Virginia, United States.

The difficult quantities to determine for radiative transfer calculations are the characteristics of the atmospheric aerosols. Fortunately, we can make reasonable assumptions regarding their values based on prior results. For example, 79 aerosol profiles have been measured at White Sands (Ref. 14) to establish an atmospheric model; the effects of aerosol complex refractive index and size distribution on extinction and absorption for the wavelength range 0.55 to 10.6 μm for desert atmospheres are reported in reference 15; and reference 16 reports that the imaginary refractive index is 0.007 at 0.6 μm and shows little dependence on wavelength over the range 0.3 to 1.1 μm.

We intend to investigate some new techniques for determining aerosol chacteristics that are under development and that make use of sky polarization measurements. We also intend to explore methods of monitoring the aerosol size distribution from inversion of the spectral optical depth measurements (Ref. 17) and aureole measurements (Ref. 18). Some of these measurements and analyses, particularly the polarimetric, fall into the research category. They represent attempts to improve the accuracy of the calibration procedure and, because of their untested nature, require validation. However, without them we anticipate an overall accuracy of about ±3% absolute. This represents an improvement over the ±5% value claimed in reference 19, and is due to our anticipated ±1% absolute accuracy of calibration of the ground instrumentation.

The proposed basic design of the instrumentation is similar to that being designed and built at the University of Arizona for the investigation of solar irradiance variations over a 23-year period. It employs a precision alt-azimuth tracking stand, with stepper motors to drive the two axes, so that it can be pointed in almost any direction or be held in alignment with the sun. A microprocessor based computer system will be used to control the motors as well as the data acquisition and processing system. A conceptual view of the instrument is shown in Fig. 5, further details of its design will be presented at the symposium.

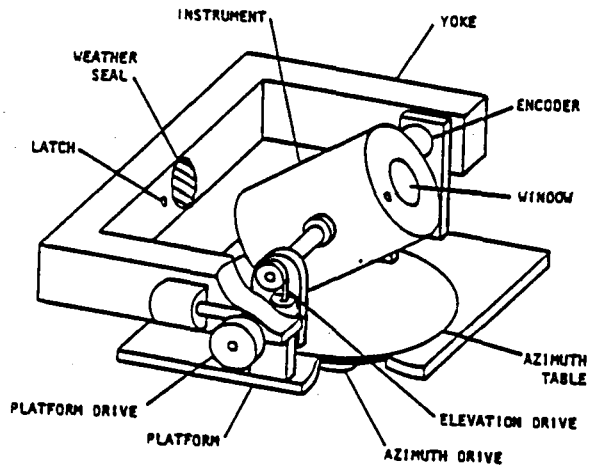

Fig. 5. Conceptual view of spectroradiometer for ground and atmospheric measurements.

6. ACKNOWLEDGEMENTS

I wish to thank J. Geist, S.J. Martinek, J.M. Palmer and E.F. Zalewski for the benefit of useful discussions. This work was supported under grant number NAG 5-196.

7. REFERENCES

1. Slater P N 1980, *Remote Sensing: Optics and Optical Systems*, Reading, Mass., Addison-Wesley, 481-484.

2. NASA Contract NAS5-23639 1977, *A study of the effects of the atmosphere on thematic mapper observations*, by Pearce W A.

3. Dave J V 1980, Effect of atmospheric conditions on remote sensing of a surface nonhomogeneity, *Photogram Eng & Remote Sensing* 46(9), 1173-1180.

4. NASA Tech Memo 83818 1981, *The effect of finite field size on classification and atmospheric correction*, by Kaufman Y J & Fraser R S.

5. Tanre D et al 1981, Influence of the background contribution on space measurements of ground reflectance, *Appl Opt.* 20(20), 3676-3684.

6. Environmental Res Inst of Michigan Final Report E77-10057 1976, *Investigation of Landsat follow-on thematic mapper spatial, radiometric and spectral resolution*, by Morgenstern J P et al.

7. Geist J 1979, Quantum efficiency of the p-n junction in silicon as an absolute radiometric standard, *Appl Opt.* 18(6), 760-762.

8. Geist J 1980, Silicon photodiode front region collection efficiency models, *J Appl Phys.* 51(7), 3993-3995.

9. Geist J et al 1979, Spectral response and self-calibration and interpolation of silicon photodiodes, *Appl Opt.* 19(22), 3795-3799.

10. Geist J & Zalewski E F 1979, The quantum yield of silicon in the visible, *Appl Phys Lett.* 35(7), 503-506.

11. Zalewski E F & Geist J 1980, Silicon photodiode absolute spectral response self-calibration, *Appl Opt.* 19(8), 1214-1216.

12. Zalewski E F 1981, private communication.

13. Kostuk R K 1981, Polarization properties of a 1000-W FEL type filament lamp, *Appl Opt.* 20(13), 2181-2184.

14. Air Force Cambridge Research Laboratories Environmental Research Papers No 285 1968, *UV visible and IR attenuation for altitudes to 50 km*, by Elterman L.

15. Jennings S G et al 1978, Effects of particulate complex refractive index and particle size distribution variations on atmospheric extinction and adsorption for visible through middle ir wavelengths, *Appl Opt.* 17(24), 3922-3929.

16. Lindberg J D & Laude L S 1974, Measurement of the absorption coefficient of atmospheric dust, *Appl Opt.* 13(8), 1923-1927.

17. King M D et al 1978, Aerosol size distribution obtained by inversion of spectral optical depth measurements, *J Atmos Sci.* 35, 2153.

18. Twitty J T 1975, The inversion of aureole measurements to derive aerosol size distributions, *J Atmos Sci.*32, 584.

19. Kriebel K T 1981, Calibration of the METEOSTAT-VIS channel by airborne measurements, *Appl Opt.* 20(1), 11-12.